STRUCTURAL SCIENCE
CRYSTAL ENGINEERING
MATERIALS

ISSN: 2052-5206
journals.iucr.org/b

Could incommensurability in sulfosalts be more common than thought? The case of meneghinite, $CuPb_{13}Sb_7S_{24}$

Luca Bindi, Václav Petříček, Cristian Biagioni, Jakub Plášil and Yves Moëlo

Acta Cryst. (2017). B**73**, 369–376

STRUCTURAL SCIENCE CRYSTAL ENGINEERING MATERIALS

ISSN 2052-5206

Could incommensurability in sulfosalts be more common than thought? The case of meneghinite, $CuPb_{13}Sb_7S_{24}$

Luca Bindi,[a] Václav Petříček,[b] Cristian Biagioni,[c]* Jakub Plášil[b] and Yves Moëlo[d]

[a]Dipartimento di Scienze della Terra, Università di Firenze, Via La Pira 4, I-50121 Firenze, Italy, [b]Institute of Physics, ASCR, Na Slovance 2, 182 21 Praha 6, Czech Republic, [c]Dipartimento di Scienze della Terra, Università di Pisa, Via Santa Maria 53, I-56126 Pisa, Italy, and [d]Institut des Matériaux Jean Rouxel, UMR 6502, CNRS, Université de Nantes, 2 rue de la Houssinière, 44322 Nantes CEDEX 3, France. *Correspondence e-mail: biagioni@dst.unipi.it

Received 24 December 2016
Accepted 15 February 2017

Edited by A. Katrusiak, Adam Mickiewicz University, Poland

Keywords: meneghinite; crystal structure; incommensurability; sulfosalt.

CCDC reference: 1533002

B-IncStrDB reference: 13202EGzpbI

Supporting information: this article has supporting information at journals.iucr.org/b

The structure of meneghinite ($CuPb_{13}Sb_7S_{24}$), from the Bottino mine in the Apuan Alps (Italy), has been solved and refined as an incommensurate structure in four-dimensional superspace. The structure is orthorhombic, superspace group $Pnma(0\beta0)00s$, cell parameters a = 24.0549 (3), b = 4.1291 (6), c = 11.3361 (16) Å, modulation vector $\mathbf{q}$ = 0.5433 (4)$\mathbf{b}^*$. The structure was refined from 6604 reflections to a final R = 0.0479. The model includes modulation of both atomic positions and displacement parameters, as well as occupational waves. The driving forces stabilizing the modulated structure of meneghinite are linked to the occupation modulation of Cu and some of the Pb atoms. As a consequence of the Cu/[] and Pb/Sb modulations, three- to sevenfold coordinations of the M cations (Pb/Sb) occur in different parts of the structure. The almost bimodal distribution of the occupation of Cu/[] and Pb/Sb at $M5$ conforms with the coupled substitution Sb^{3+} + [] → Pb^{2+} + Cu^{+}, thus corroborating the hypothesis deduced previously for the incorporation of copper in the meneghinite structure. The very small departure (∼0.54 *versus* 0.50) from the commensurate value of the modulation raises the question of whether other sulfosalts considered superstructures have been properly described, and, in this light, if incommensurate modulation in sulfosalts could be much more common than thought.

1. Introduction

The recent development of aperiodic crystallography has led to the discovery of several incommensurate crystals, and indicated that incommensurability cannot be neglected in any field of solid-state chemistry. Indeed, incommensurate modulation has been found in almost all different families of structures that include synthetic inorganic and organic compounds, as well as proteins (Janssen *et al.*, 2007; van Smaalen, 2007). Modulated structures have also been widely found in various minerals, although their structural analysis is still strongly underdeveloped. Indeed, it is not common to find minerals with strong and sharp satellites related to an aperiodic structure to be used for a structural refinement with superspace formalism. Nevertheless, there are several minerals which have incommensurate satellites visible with electron diffraction including: clinopyroxenes (kosmochlor–diopside join; Sakamoto *et al.*, 2003), quartz (*e.g.* Heaney & Veblen, 1991), feldspars (*e.g.* Yamamoto *et al.*, 1984; Steurer & Jagodzinski, 1988; Kalning *et al.*, 1997; Sanchez-Munoz *et al.*, 1998), melilite (Bindi *et al.*, 2001, and references therein), fresnoite (Bindi *et al.*, 2006), cancrinite–sodalite join (*e.g.* Hassan & Buseck, 1989, 1992; Xu & Veblen, 1995; Hassan,

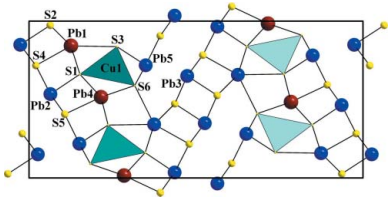

2000; Hassan *et al.*, 2004; Bolotina, 2006; Bolotina *et al.*, 2006), nepheline (Withers *et al.*, 1998; Angel *et al.*, 2008; Friese *et al.*, 2011), lazurite (Rastsvetaeva *et al.*, 2002; Bolotina *et al.*, 2003*a*, 2003*b*, 2004), tridymite (*e.g.* Pryde & Dove, 1998) and mullite (Angel *et al.*, 1991). Incommensurate modulations can also be found among sulfides, tellurides and sulfosalts including bornite (Buseck & Cowley, 1983), pyrrhotite (Li & Franzen, 1996), calaverite (*e.g.* Schutte & de Boer, 1988; Caracas & Gonze, 2001), sylvanite (Krutzen & Inglesfield, 1990), rickardite (Schutte & de Boer, 1993), muthmannite (Bindi, 2008), proustite (Subramanian *et al.*, 2000), the cylindrite–franckeite series (Evain *et al.*, 2006; Makovicky *et al.*, 2008, 2011), lengenbachite (Makovicky & Hyde, 1981; Makovicky *et al.*, 1994), the pearceite–polybasite series (Withers *et al.*, 2008; Bindi *et al.*, 2013), and sartorite (Pring *et al.*, 1993). Among sulfosalts, however, only the incommensurate structures of levyclaudite (Evain *et al.*, 2006) and franckeite (Makovicky *et al.*, 2011) have been studied by means of a multidimensional crystal structure refinement. The paucity of these studies, together with the fact that sulfosalts are widespread in nature, could hide some heretofore unknown structural complexities.

Sulfosalts are complex chalcogenides with the formula $A_xB_yC_z$, where A = Pb, Cu, Ag, Hg, Tl, Fe, Mn, Sn^{2+}, Sn^{4+} and other metals, B = As, Sb and Bi in fundamentally threefold coordination, and $C = S^{2-}$, Se^{2-} and Te^{2-} (Makovicky, 1997). Their crystal structures can be described as formed by rods, blocks or layers of simple archetypal structures (*e.g.* PbS, SnS) variously recombined. Among the SnS-archetype-based sulfosalts, the members of the accretional homologous series of meneghinite (Makovicky, 1985) exhibit a crystal structure made up of slices of SnS-like structure. Aikinite ($CuPbBiS_3$; Chapman, 1843) and meneghinite ($CuPb_{13}Sb_7S_{24}$; Bechi, 1852) are the oldest members of this series, and were always described with a unit cell having one of the crystallographic axes of about 4 Å. The unit cell of most SnS-archetype- and PbS-archetype-based sulfosalts is characterized by such a periodicity that can be commonly found doubled, giving rise to 8 Å commensurate superstructures.

The crystal structure of meneghinite was solved by Euler & Hellner (1960) using a sample from the Bottino mine (Tuscany, Italy). These authors were able to solve only the 4 Å structure, observing the occurrence in the oscillation photographs of very faint layer lines between the zero line and the strong line representing the 4.128 Å periodicity. According to these authors, the actual superstructure of meneghinite should have a 24 × 4.128 Å periodicity and the weak layer lines could correspond to the 11th and 13th order of reflections. As a matter of fact, with very long exposures they were not able to find any of the missing layer lines. Similar features were reported by Hicks & Nuffield (1978) in meneghinite from Ontario, Canada. In contrast, Cu-free synthetic meneghinite did not show any additional superstructure reflections. According to Hicks & Nuffield (1978), the appearance of the faint layer lines results from some ordering of Pb and Sb. Finally, Moëlo *et al.* (2002) reported a chemical and structural study of a Cu-poor meneghinite from La Lauzière Massif (Savoie, France). These authors refined the crystal structure in the same orthorhombic symmetry (space group *Pnma*) and with the same unit cell [a = 24.080 (5), b = 4.1276 (8), c = 11.369 (2) Å, V = 1130.0 (4) $Å^3$, Z = 4] as Euler & Hellner (1960), but showed a significantly lower site-occupancy factor for the tetrahedral Cu site (0.146 *versus* 0.25).

Here we report the finding of a meneghinite crystal with additional weak reflections leading to an apparent doubling of the 4 Å periodicity. A careful inspection of the position of the additional reflections indicated that they are actually incommensurate with the lattice periodicity (being slightly displaced from the $\frac{1}{2}$ position) (Fig. 1); these reflections correspond to the layer lines described by Euler & Hellner (1960) and Hicks & Nuffield (1978) and interpreted as due to a commensurate superstructure. The very small departure (∼0.54 *versus* 0.50) from the commensurate value raises the question: could several sulfosalts previously considered superstructures have been properly solved and refined? Indeed, even if the 8 Å periodicity is a natural consequence of the trapezoidal cross sections of many As-, Sb- and sometimes Bi-coordination polyhedra, more complex superstructures are commonly reported for the minerals of the sulfosalt realm. These could indeed represent only approximations and the problems usually encountered in their solutions/refinements (*e.g.* partially occupied sites, structural disorder, large displacement parameters) could be due to the fact that the structure was forced to be commensurate.

2. Experimental

2.1. Sample occurrence and chemical data

The sample of meneghinite used in the present study is from the Pb–Zn–Ag Bottino mine in the Apuan Alps (Tuscany, Italy). The sample was represented by a loose crystal, 2 cm in length and 1 cm in thickness, collected in 2005 from the Redola level, one of the ancient mining works of the mine. Meneghinite occurred in a vug of a quartz vein, in association with chalcopyrite, Fe-bearing dolomite and siderite.

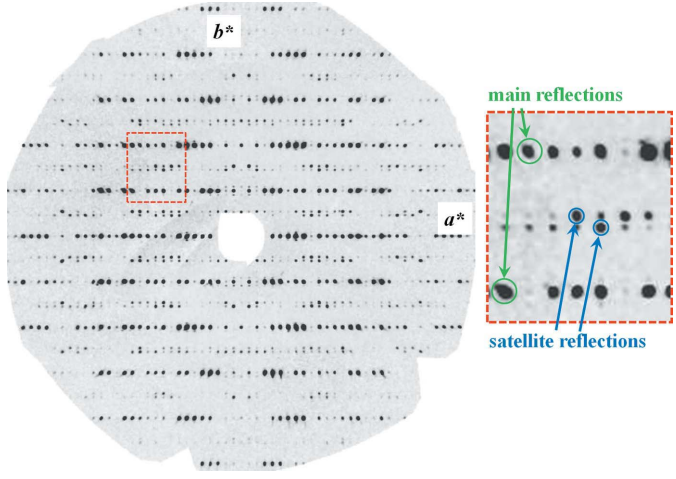

Figure 1
Reconstructed precession photograph on $hk\bar{2}$ reciprocal lattice layer for meneghinite. Main and satellite reflections are indicated in the inset.

Table 1
Chemical data and formulae for meneghinite.

Chemical data is in wt% (average of three spot analyses) and chemical formulae on the basis of Σ(Pb + Sb) = 20 atoms per formula unit (apfu).

Element	Average	E.s.d.	Atom	Apfu	E.s.d.	Probe standard	WDS line
Cu	1.45	0.02	Cu	0.99	0.01	Cu metal	Cu *Kα*
Ag	0.07	0.04	Ag	0.03	0.02	Ag metal	Ag *Lα*
Pb	62.32	0.22	Pb	13.07	0.01	PbS	Pb *Mα*
Sb	19.40	0.09	Sb	6.93	0.03	Stibnite	Sb *Lα*
S	17.59	0.05	S	23.85	0.15	Pyrite	S *Kα*
Se	0.11	0.05	Se	0.06	0.03	Se element	Se *Lα*
Total	100.94	0.23	Ev†	0.3	0.6		

† Relative error on valence equilibrium (%), calculated as $[\sum(\text{val}+) - \sum(\text{val}-)] \times 100/\sum(\text{val}-)$.

Quantitative chemical analyses of meneghinite from the Bottino mine were carried out using a CAMECA SX100 electron microprobe (*Microsonde Ouest* laboratory, IFREMER, Plouzané, France). The operating conditions were: accelerating voltage 20 kV, beam current 20 nA, beam size ≃ 1 μm. The studied grain was very homogeneous ($n = 3$). Chemical data are given in Table 1. Compared with the ideal formula of $CuPb_{13}Sb_7S_{24}$, the chemical formula of the meneghinite from the Bottino mine in Italy is $(Cu_{0.99}Ag_{0.03})_{\Sigma 1.02}Pb_{13.07}Sb_{6.93}(S_{23.85}Se_{0.06})_{\Sigma 23.91}$.

2.2. Single-crystal X-ray diffraction study

The intensity data were collected from a meneghinite crystal (size: 0.14 × 0.07 × 0.06 mm), obtained by crushing a piece of a larger crystal, using a Rigaku (Oxford Diffraction) SuperNova single-crystal diffractometer equipped with an Atlas S2 CCD detector utilizing Mo *Kα* radiation, which was provided by a microfocus X-ray tube and monochromated by primary mirror optics. The *ω* rotational scans (frame width 1.0°, counting time 150 seconds per frame) were adopted for the acquisition of the three-dimensional intensity data. From the total of 70 366 reflections, 6604 were independent and 4696 classified as unique observed with $I > 3\sigma(I)$. Among these, 1473 were main reflections, 2577 first-order satellites, and 2554 second-order satellites. Corrections for background, Lorentz effects and polarization were applied during data reduction in *CrysAlis* software; a correction for absorption, using Gaussian integration ($\mu = 54.56$ mm^{-1}), was applied in *JANA*2006 (Petříček *et al.*, 2014) to the data leading to $R_{int} = 0.045$. Table 2 shows the experimental details.

2.3. Superspace structure refinement

All calculations related to the structure refinement have been performed with the *JANA*2006 system of programs (Petříček *et al.*, 2014). The experimental data collection obtained at room temperature revealed systematic extinctions unequivocally defining the *Pnma*(0*β*0)00*s* superspace group. As the meneghinite structure is well known, we used the fractional coordinates of atoms reported by Moëlo *et al.* (2002) as a starting model in our refinement. The refinement of the modulated structure was straightforward. The only problem encountered was the partially occupied position of the Cu atom as well as two mixed sites Pb3/Sb3 and Pb5/Sb5. The occupational and substitutional modulation waves lead to an almost perfect separation of Cu/[] and Pb/Sb positions. That was the reason why two modulation models were tested. One with a full use of crenel functions (Petříček *et al.*, 1995, 2016) and a second based on harmonic functions. It turned out that the harmonic model leads to a significantly better fit. Therefore, it suggests that in the crystal there are Pb-rich and Sb-rich domains, but the boundaries between them are not sharp. The same mechanism is valid for regions where Cu atoms are present.

Positional parameters, occupational waves and atomic displacement parameters are given as supplementary tables. Bond distances are reported in Table 3.

Table 2
Experimental details.

Crystal data	
Chemical formula	$CuPb_{13}Sb_7S_{24}$
M_r	4393.3
Cell setting, superspace group	Orthorhombic, *Pnma*(0*β*0)00*s*
Temperature (K)	297
Wavevector	**q** = 0.5433 (4)**b***
a, *b*, *c* (Å)	24.0549 (3), 4.1291 (6), 11.3361 (16)
V (Å^3)	1126.0 (2)
Z	1
Radiation type	Mo *Kα*
μ (mm^{-1})	54.69
Data collection	
Diffractometer	SuperNova Rigaku (Oxford Diffraction)
No. of measured, independent and observed [$I > 3\sigma(I)$] reflections	70 366, 6604, 4696
No. of main reflections	1473
No. of first-order satellite reflections	2577
No. of second-order satellite reflections	2554
R_{int}	0.045
Refinement	
Refinement on	F^2
R, *wR* (all reflections)	0.0479, 0.1076
R, *wR* (main reflections)	0.0252, 0.0622
R, *wR* (satellites)	
First order	0.0490, 0.0979
Second order	0.1725, 0.3047
S	1.197
No. of reflections	6604
No. of parameters	216
$\Delta\rho_{max}$, $\Delta\rho_{min}$(e Å^{-3})	1.66, −1.58
Extinction correction	None
Source of atomic scattering factors	*International Tables for Crystallography* (Wilson, 1992)

Computer programs: *JANA*2006 (Petříček *et al.*, 2014).

3. Results and discussion

The average structure of meneghinite (Fig. 2) can be described as made up of (501) or ($\bar{5}$01) slices of SnS-like structure. The surface of these slices form wavy composition planes on which the two adjacent slices face each other and are mutually

Table 3
Selected bond distances (Å) in the modulated structure of meneghinite.

	Average	Minimal	Maximal
Cu1—S1^{ii}	2.41 (8)	2.39 (13)	2.45 (13)
Cu1—S3^{iii}	2.36 (8)	2.29 (9)	2.52 (9)
Cu1—S3	2.37 (8)	2.29 (9)	2.52 (9)
Cu1—S6	2.42 (9)	2.29 (13)	2.48 (13)
Pb1—S1^{iii}	2.988 (3)	2.949 (4)	3.042 (4)
Pb1—S1	2.988 (3)	2.949 (4)	3.042 (4)
Pb1—S2^{iv}	2.939 (3)	2.859 (4)	2.987 (4)
Pb1—S2^{v}	2.939 (3)	2.859 (4)	2.987 (4)
Pb1—S4^{iv}	2.901 (4)	2.891 (6)	2.907 (6)
Pb1—S3^{x}	3.319 (4)	3.163 (6)	3.430 (6)
Pb1—S6	3.148 (4)	3.095 (7)	3.208 (7)
Pb2—S1	2.587 (3)	2.445 (6)	2.673 (6)
Pb2—S4^{iv}	3.044 (4)	2.890 (5)	3.342 (5)
Pb2—S4^{v}	3.045 (4)	2.890 (5)	3.337 (5)
Pb2—S5	2.802 (4)	2.496 (4)	2.983 (4)
Pb2—S5^{vi}	2.803 (4)	2.490 (4)	2.983 (4)
Pb2—S4^{viii}	3.503 (3)	3.489 (6)	3.527 (6)
Sb2—S1	2.529 (3)	2.411 (6)	2.660 (6)
Sb2—S5	2.684 (4)	2.427 (4)	2.982 (4)
Sb2—S5^{vi}	2.686 (4)	2.427 (4)	2.983 (4)
Pb3—S2	2.597 (3)	2.462 (6)	2.680 (6)
Pb3—S2^{iv}	3.010 (3)	2.936 (4)	3.199 (4)
Pb3—S2^{v}	3.010 (3)	2.936 (4)	3.200 (4)
Pb3—S4^{iii}	2.838 (4)	2.517 (4)	3.013 (4)
Pb3—S4	2.838 (4)	2.520 (4)	3.013 (4)
Pb3—S5^{i}	3.489 (4)	3.458 (7)	3.514 (7)
Sb3—S2	2.544 (3)	2.438 (6)	2.665 (6)
Sb3—S4^{iii}	2.717 (4)	2.452 (4)	2.993 (4)
Sb3—S4	2.717 (4)	2.452 (4)	2.994 (4)
Pb4—S1^{iii}	3.037 (3)	2.890 (4)	3.137 (4)
Pb4—S1	3.037 (3)	2.890 (4)	3.136 (4)
Pb4—S3^{vii}	2.948 (4)	2.830 (4)	3.076 (4)
Pb4—S3^{viii}	2.947 (4)	2.830 (4)	3.076 (4)
Pb4—S5	2.893 (4)	2.843 (6)	2.953 (6)
Pb4—S3^{x}	3.811 (4)	3.536 (6)	3.964 (6)
Pb4—S6^{xi}	3.291 (4)	3.076 (5)	3.481 (5)
Pb4—S6^{x}	3.290 (4)	3.076 (5)	3.481 (5)
Pb5—S3	2.519 (4)	2.429 (6)	2.596 (6)
Pb5—S5^{i}	3.047 (4)	2.894 (5)	3.284 (5)
Pb5—S5^{ix}	3.045 (4)	2.894 (5)	3.280 (5)
Pb5—S6	2.781 (4)	2.532 (5)	2.996 (5)
Pb5—S6^{vi}	2.780 (4)	2.529 (5)	2.996 (5)
Pb5—S2^{v}	3.464 (4)	3.429 (6)	3.505 (6)
Sb5—S3	2.481 (4)	2.419 (6)	2.596 (6)
Sb5—S6	2.658 (4)	2.411 (5)	2.996 (5)
Sb5—S6^{vi}	2.658 (4)	2.411 (5)	2.996 (5)

Symmetry codes: (i) $x, y, z-1$; (ii) $-x+\frac{1}{2}, -y+1, z-\frac{1}{2}$; (iii) $x, y-1, z$; (iv) $-x, y-\frac{1}{2}, -z$; (v) $-x, y+\frac{1}{2}, -z$; (vi) $x, y+1, z$; (vii) $x, y-1, z+1$; (viii) $x, y, z+1$; (ix) $x, y+1, z-1$; (x) $-x+\frac{1}{2}, -y+1, z+\frac{1}{2}$; (xi) $-x+\frac{1}{2}, -y, z+\frac{1}{2}$.

related by an *n*-glide plane parallel to (010) of meneghinite. Tetrahedral coordination sites in the wavy interface can be occupied by Cu atoms according to the coupled substitution $Cu^{+} + Pb^{2+} \rightarrow [] + Sb^{3+}$.

In the structure there are six metal sites, Cu and Pb1 to Pb5, and six S atoms (S1 to S6). The Cu position is partially occupied, Pb1 and Pb4 are fully occupied by Pb and Pb2, Pb3 and Pb5 show variable Sb contents replacing Pb. The most relevant variations observed as a function of the fourth (*t*) coordinate in superspace concern the Cu and Pb2, Pb3, and Pb5 polyhedra. The Cu position shows a strong occupation modulation (Fig. 3), almost bimodal, with regions where the corresponding polyhedron is empty (Cu has been refined *versus* structural vacancy). This reflects very well on the variation of bond distances as a function of the fourth coordinate in superspace, which range from 2.32 Å (Cu-rich regions) to 2.49 Å (Cu-poor regions). It is noteworthy that we observed an almost regular alternation along the *b* axis of large and small tetrahedra (Fig. 4*a*). The occupation modulation observed for Pb2 (refined *versus* Sb) points to regions almost totally enriched in Sb at $t \sim 0.35$ (Fig. 5*a*). The corresponding bond distances (Fig. 5*b*) and bond valence sums (BVS; Fig. 5*c*), which show a jump to about 4.6 valence units (v.u.) from the value of 2.00 v.u., are in excellent agreement with this site distribution (in particular the value of 4.6 v.u. and in general the value of >3.0 v.u. have to be considered for Pb^{2+} atoms in an essentially Sb^{3+}-dominated polyhedron). Indeed, at $t \sim 0.35$, three *M*2—S bonds show a shortening to a mean bond distances of 2.63 Å and two *M*2—S bonds are too long to be considered still bonded to *M*2 (Fig. 5*b*). This feature can be

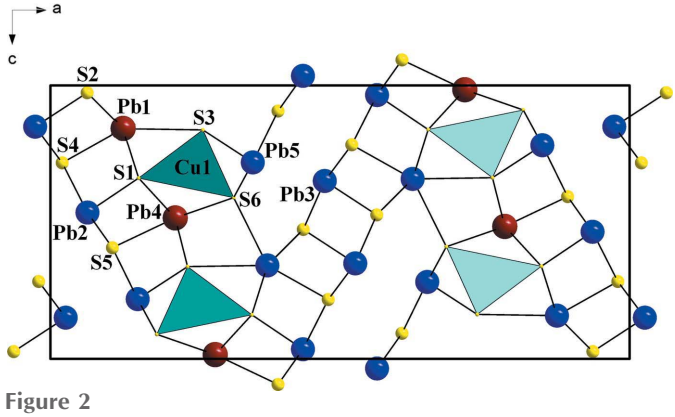

Figure 2
The average structure of meneghinite down [010]. Cu atoms are drawn as light-blue tetrahedra. Red, blue and yellow spheres correspond to Pb, Pb/Sb and S atoms, respectively. The unit cell and the orientation of the figure are outlined.

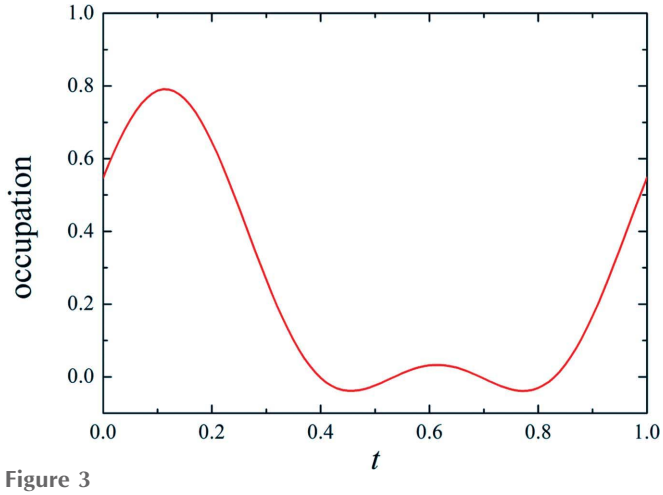

Figure 3
Occupation modulation of the Cu atom as a function of the fourth coordinate (*t*) in superspace. Refined cation population at the site: $Cu_{0.24}[]_{0.76}$.

observed in Fig. 4(*b*) where two consecutive Pb2/Sb2 atoms in the modulated structure of meneghinite are seen along the *b* axis. Such an environment is characteristic for the stereochemical activity of the lone pair of electrons of Sb^{3+} atoms, which usually give rise to (3 + 2)-coordination polyhedra in sulfosalts (*e.g.* Ferraris *et al.*, 2008). Similar considerations can be made for Pb3 (refined *versus* Sb), which shows regions almost totally enriched in Sb at $t \sim 0.62$ (Fig. 6*a*), with corresponding shorter bond distances (Fig. 6*b*) and higher BVS (Fig. 6*c*). The only slight difference of the Pb3 position with respect to Pb2 is related to a more regular distribution of the bond distances when the polyhedra are dominated by lead (Fig. 4*c*). More complex is the behavior of Pb5, which is the structural site with the higher concentration of Sb. The Sb-for-Pb substitution (Fig. 7*a*) seems to show a bimodal distribution as a function of the fourth coordinate in the superspace, with Pb enrichments in the *t* range of 0.10–0.60. To some extent, it resembles what is observed for the Cu modulation, but it is shifted along *t*. Indeed, we observed an almost regular alternation along the *b* axis of Pb- and Sb-dominated polyhedra in the modulated structure (Fig. 4*d*). The variation of the *M*5—S bond distances (Fig. 7*b*) and of BVS (Fig. 7*c*) agrees well with the Pb/Sb distribution at the site, with shorter bonds and higher BVS where Sb is the dominant cation. Pb1 (Fig. 8) and Pb4 (Fig. 9), fully occupied by Pb, exhibit more regular polyhedra as a function of the fourth coordinate in superspace, and their BVS are always close to 2.00 v.u.

The general structural characteristics described above indicate that the driving forces stabilizing the modulated

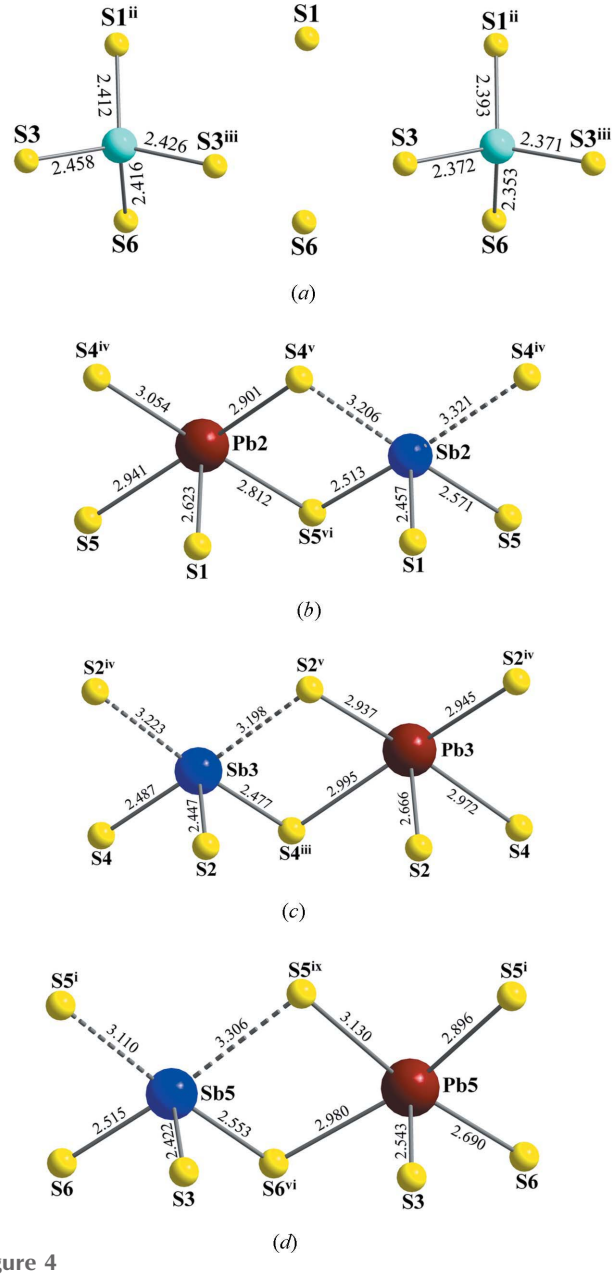

Figure 4
Coordination environments of Cu1 (*a*), Pb2/Sb2 (*b*), Pb3/Sb3 (*c*) and Pb5/Sb5 (*d*) along the *b* axis in the modulated structure of meneghinite. Atom colours as in Fig. 2. The *b* axis is horizontal. Bond distances are given in Å.

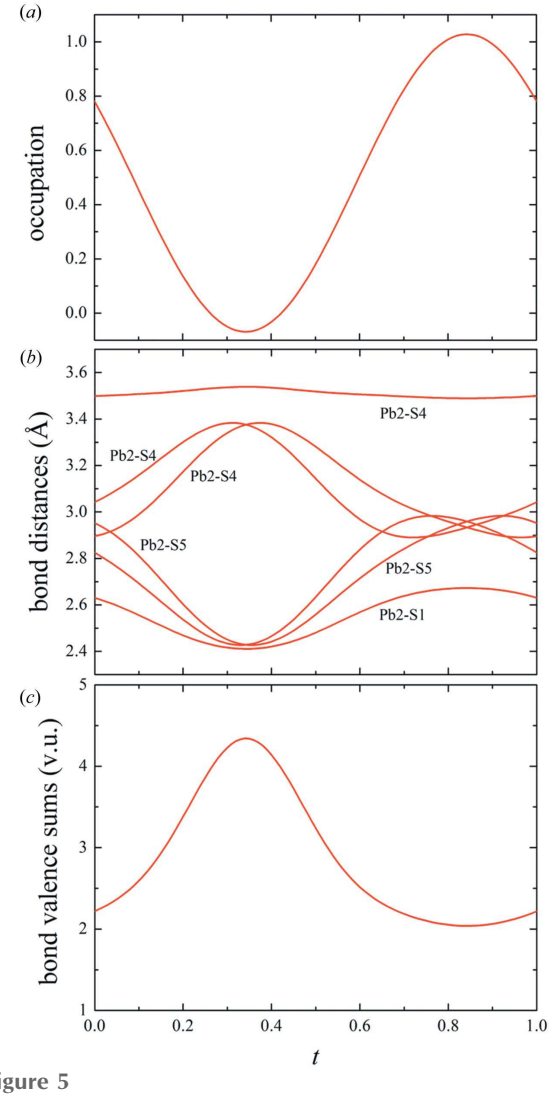

Figure 5
Occupation modulation (*a*), bond distances (*b*) and bond valence sums (*c*) of the Pb2/Sb2 atom as a function of the fourth coordinate (*t*) in superspace. Values >3.0 v.u. have to be considered for Pb^{2+} atoms in essentially Sb^{3+}-dominated polyhedra. Refined cation population at the site: $Pb_{0.48}Sb_{0.52}$.

structure of meneghinite are linked to the occupational modulation of Cu and some of the Pb atoms. Especially interesting is what happens to the Pb atoms when replaced by Sb. The considerable difference in size between Pb^{2+} and Sb^{3+} [although we are dealing with a highly covalent structure with very asymmetric coordinations, for the sake of clarity we compare the ionic radii of Pb^{2+} = 1.19 and Sb^{3+} = 0.76 Å; values taken from Shannon (1976)] provokes a continuous change in the coordination polyhedra as a function of the fourth coordinate in superspace (Fig. 4), which causes the presence of three- to sixfold coordinations of the *M* cations (Pb/Sb) in different portions of the modulated structure. Although the change in coordination is clearly evident (Fig. 4), the deformation of the structure is not marked, as the modulation in meneghinite mainly involves the occupation of the structural sites, with minor effects on the positions of the atoms and their atomic displacement parameters. The almost bimodal and similar distribution of the occupation of Cu/[] and Pb/Sb at *M*5 is in agreement with the hypothesized coupled substitution $Sb^{3+} + [] \rightarrow Pb^{2+} + Cu^{+}$ (Moëlo *et al.*, 2002), which shows the reason for the incorporation of copper in the meneghinite structure.

4. Outlook

The introduction of area detectors in the 1990s has brought some revolutionary improvements into the data collection time, ease of diffractometer operation, and sensitivity. Furthermore, the recent availability of very powerful CCD detectors and software has brought a significant revolution into aperiodic crystallography, enabling researchers to work with very small samples having complicated structures

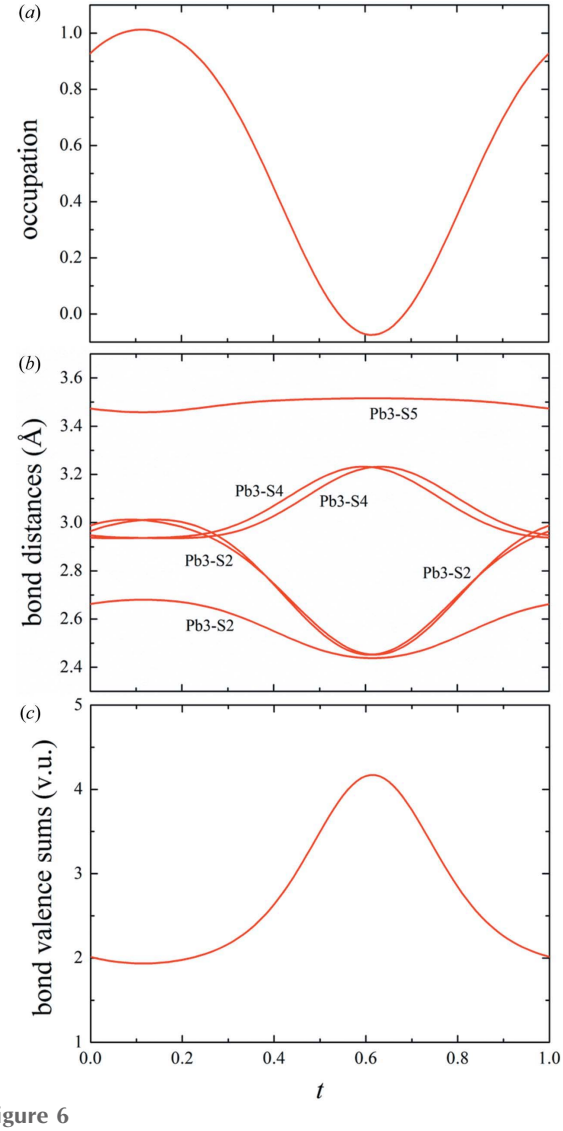

Figure 6
Occupation modulation (*a*), bond distances (*b*) and bond valence sums (*c*) of the Pb3/Sb3 atom as a function of the fourth coordinate (*t*) in superspace. Values >3.0 v.u. have to be considered for Pb^{2+} atoms in essentially Sb^{3+}-dominated polyhedra. Refined cation population at the site: $Pb_{0.52}Sb_{0.48}$.

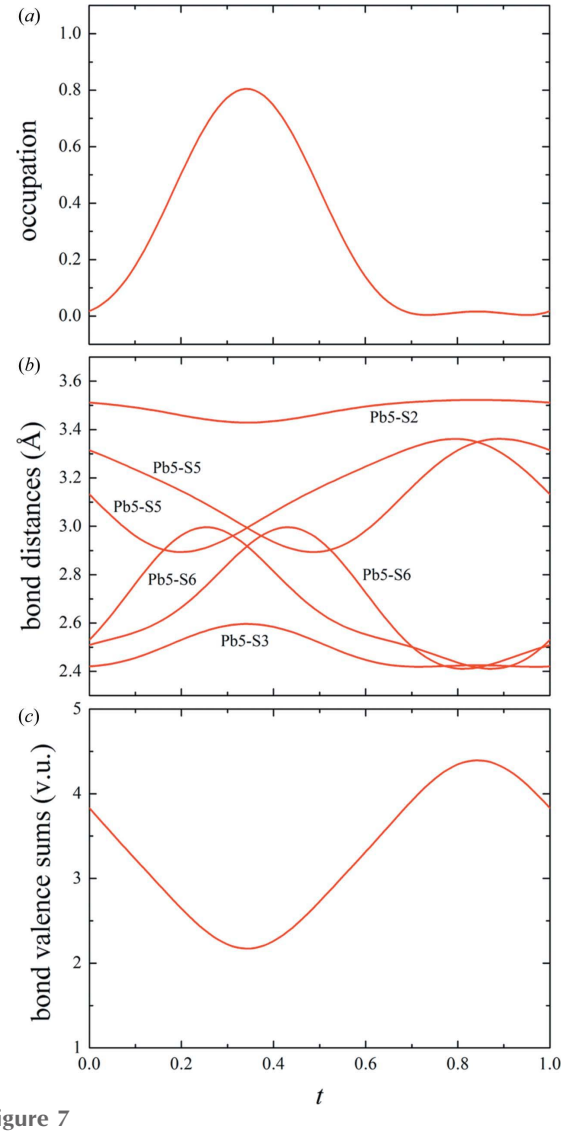

Figure 7
Occupation modulation (*a*), bond distances (*b*) and bond valence sums (*c*) of the Pb5/Sb5 atom as a function of the fourth coordinate (*t*) in superspace. Values >3.0 v.u. have to be considered for Pb^{2+} atoms in essentially Sb^{3+}-dominated polyhedra. Refined cation population at the site: $Pb_{0.28}Sb_{0.72}$.

(Chapuis & Arakcheeva, 2013; Pina & López-Acevedo, 2016). Unfortunately, all these great advantages have been accompanied by a turning of the diffractometer more into a black box that operates in a push-button mode. This mode usually works very well with most of the periodic inorganic structures, but it is definitely not adequate for experiments involving samples exhibiting incommensurate structures. For this reason, several incommensurate structures belonging to the mineral kingdom could have been inadequately characterized, or, much more likely, been considered commensurate even if they were not. A very clever example of the procedure that should be followed for complex cases is that adopted by Petříček & Makovicky (2006) for the study of selected members (gladite, salzburgite, paarite and krupkaite) of the bismuthinite–aikinite (Bi_2S_3–$CuPbBiS_3$) series. Although these structures are real superstructures, they were refined as commensurately modulated structures using the superspace approach in the superspace group $Pmcn(0\beta0)00s$ with β assuming the value of $\frac{1}{3}$, $\frac{1}{4}$, $\frac{1}{5}$ and 2. The case of meneghinite presented here is a clear example of how a complex incommensurate structure was considered a commensurate one (*e.g.* Euler & Hellner, 1960; Hicks & Nuffield, 1978). An eventual refinement of the 'forced' commensurate structure, would have not allowed (i) the understanding of the real driving forces causing the appearance of the observed satellite reflections, (ii) the actual global adjustments of the structure framework, and (iii) the overall positional (or displacement, occupancy) trends, which remain usually submerged in localized descriptions. Similar problems could be encountered if one had refined meneghinite as an elevenfold commensurate superstructure [given the fact that 6/11 = 0.5454, very close to the incommensurate component of the modulation wavevector along **b***, *i.e.* 0.5433 (4)] in three-dimensional physical space. The superspace approach is indeed intended to allow the study of the continuous variations of a modulated structure as a function of the additional dimensions in the superspace and reveal the global adjustments of the structure framework.

Acknowledgements

This research received support by the University of Florence, 'Progetto di Ateneo 2014' issued to LB and by MIUR through project *SIR* 2014 'THALMIGEN – Thallium: Mineralogy, Geochemistry, and Environmental Hazards' granted to CB. The crystallographic part was supported by the project 14-03276S of the Czech Science Foundation using instruments of the ASTRA Lab established within the Operation program Prague Competitiveness – project CZ.2.16/3.1.00/24510. Thoughtful comments by Emil Makovicky and two anonymous reviewers were very helpful to improve the quality of the paper.

Funding information

Funding for this research was provided by: University of Florence, 'Progetto di Ateneo 2014'; Ministero dell'Istruzione, dell'Università e della Ricerca (award No. SIR 2014 Grant No.

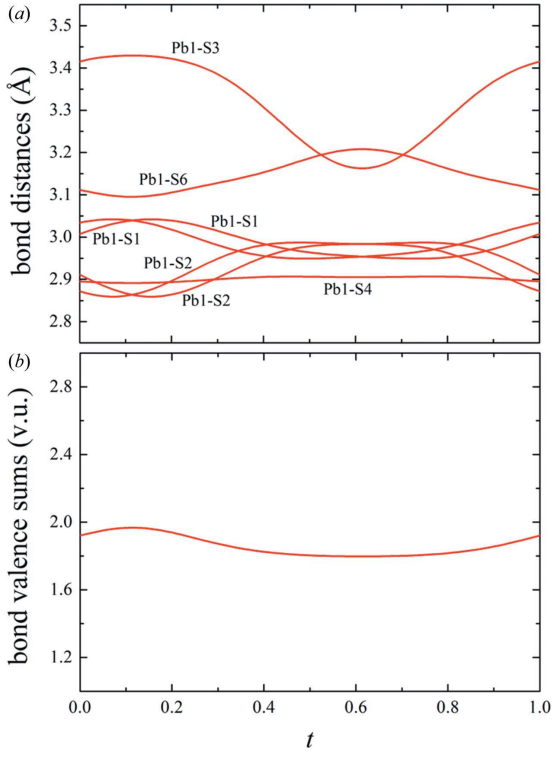

Figure 8
Bond distances (*a*) and bond valence sums (*b*) of the Pb1 atom as a function of the fourth coordinate (*t*) in superspace.

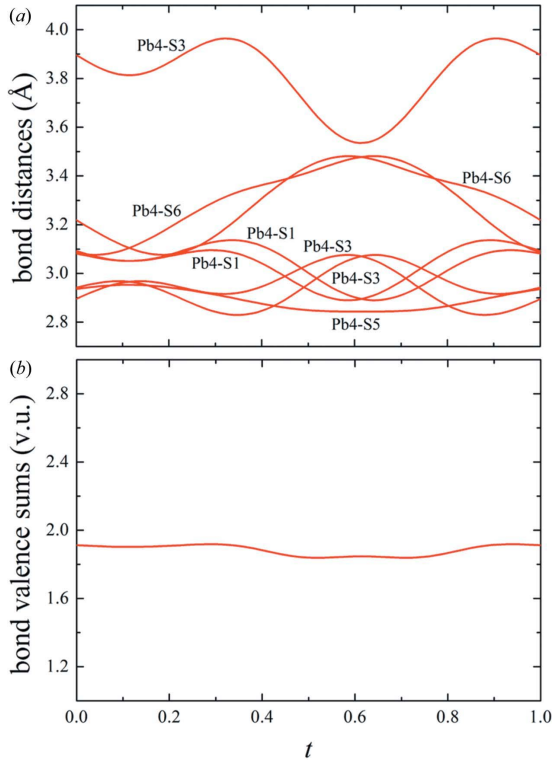

Figure 9
Bond distances (*a*) and bond valence sums (*b*) of the Pb4 atom as a function of the fourth coordinate (*t*) in superspace.

RBSI14A1CV); Czech Science Foundation (award No. 14-03276S).

References

Angel, R. J., Gatta, G. D., Ballaran, T. B. & Carpenter, M. (2008). *Can. Mineral.* **46**, 1465–1476.

Angel, R. J., McMullan, R. K. & Prewitt, C. T. (1991). *Am. Mineral.* **76**, 332–342.

Bechi, E. (1852). *Atti R. Accad. Georg.* **30**, 84–87. (In Italian.)

Bindi, L. (2008). *Philos. Mag. Lett.* **88**, 533–541.

Bindi, L., Bonazzi, P., Dušek, M., Petříček, V. & Chapuis, G. (2001). *Acta Cryst.* B**57**, 739–746.

Bindi, L., Dusek, M., Petricek, V. & Bonazzi, P. (2006). *Acta Cryst.* B**62**, 1031–1037.

Bindi, L., Schaper, A. K., Kurata, H. & Menchetti, S. (2013). *Am. Mineral.* **98**, 1279–1284.

Bolotina, N. B. (2006). *Crystallogr. Rep.* **51**, 968–976.

Bolotina, N. B., Rastsvetaeva, R. K., Chapuis, G., Schönleber, A., Sapozhnikov, A. N. & Kashaev, A. A. (2004). *Ferroelectrics*, **305**, 95–98.

Bolotina, N. B., Rastsvetaeva, R. K. & Sapozhnikov, A. N. (2006). *Crystallogr. Rep.* **51**, 589–595.

Bolotina, N. B., Rastsvetaeva, R. K., Sapozhnikov, A. N., Kashaev, A. A., Shönleber, A. & Chapuis, G. (2003*a*). *Crystallogr. Rep.* **48**, 721–727.

Bolotina, N. B., Rastsvetaeva, R. K., Sapozhnikov, A. N., Kashaev, A. A., Schöenleber, A. & Chapuis, G. (2003*b*). *Crystallogr. Rep.* **48**, 8–11.

Buseck, P. R. & Cowley, J. M. (1983). *Am. Mineral.* **68**, 18–40.

Caracas, R. & Gonze, X. (2001). *Acta Cryst.* B**57**, 633–637.

Chapman, E. J. (1843). *Practical Mineralogy*, p. 127. London: Hippolyte Bailliere.

Chapuis, G. & Arakcheeva, A. (2013). *R. Fis. Acc. Lincei*, **24**, 77–84.

Euler, R. & Hellner, E. (1960). *Z. Kristallogr.* **113**, 345–372.

Evain, M., Petricek, V., Moëlo, Y. & Maurel, C. (2006). *Acta Cryst.* B**62**, 775–789.

Ferraris, G., Makovicky, E. & Merlino, S. (2008). *Crystallography of Modular Materials*. Oxford University Press, 370 pp.

Friese, K., Grzechnik, A., Petříček, V., Schönleber, A., van Smaalen, S. & Morgenroth, W. (2011). *Acta Cryst.* B**67**, 18–29.

Hassan, I. (2000). *Am. Mineral.* **85**, 1383–1389.

Hassan, I., Antao, S. M. & Parise, J. B. (2004). *Mineral. Mag.* **68**, 499–513.

Hassan, I. & Buseck, P. R. (1989). *Am. Mineral.* **74**, 394–410.

Hassan, I. & Buseck, P. R. (1992). *Can. Mineral.* **30**, 49–59.

Heaney, P. J. & Veblen, D. R. (1991). *Am. Mineral.* **76**, 1018–1032.

Hicks, W. D. & Nuffield, E. W. (1978). *Can. Mineral.* **16**, 393–395.

Janssen, T., Chapuis, G. & de Boissieu, M. (2007). *Aperiodic Crystals, from Modulated Phases to Quasicrystals*. Oxford University Press.

Kalning, M., Dorna, V., Press, W., Kek, S. & Boysen, H. (1997). *Z. Kristallogr.* **212**, 545–549.

Krutzen, B. C. H. & Inglesfield, J. E. (1990). *J. Phys. Condens. Matter*, **2**, 4829–4847.

Li, F. & Franzen, H. F. (1996). *J. Solid State Chem.* **126**, 108–120.

Makovicky, E. (1985). *Fortschr. Miner.* **63**, 45–89.

Makovicky, E. (1997). *EMU Notes Mineral.* **1**, 237–271.

Makovicky, E. & Hyde, B. G. (1981). *Struct. Bond.* **46**, 103–105.

Makovicky, E., Leonardsen, E. & Moëlo, Y. (1994). *Neues Jahr. Miner. Abh.* **166**, 169–191.

Makovicky, E., Petříček, V., Dušek, M. & Topa, D. (2008). *Am. Mineral.* **93**, 1787–1798.

Makovicky, E., Petříček, V., Dušek, M. & Topa, D. (2011). *Am. Mineral.* **96**, 1686–1702.

Moëlo, Y., Palvadeau, P., Meisser, N. & Meerschaut, A. (2002). *C. R. Geosci.* **334**, 529–536.

Petříček, V., Dušek, M. & Palatinus, L. (2014). *Z. Kristallogr.* **229**, 345–352.

Petříček, V., Eigner, V., Dušek, M. & Čejchan, A. (2016). *Z. Kristallogr.* **231**, 301–312.

Petříček, V. & Makovicky, E. (2006). *Can. Mineral.* **44**, 189–206.

Petříček, V., van der Lee, A. & Evain, M. (1995). *Acta Cryst.* A**51**, 529–535.

Pina, C. M. & López-Acevedo, V. (2016). *Crystals*, **6**, 137.

Pring, A., Williams, T. & Withers, R. (1993). *Am. Mineral.* **78**, 619–626.

Pryde, A. K. A. & Dove, M. T. (1998). *Phys. Chem. Miner.* **26**, 171–179.

Rastsvetaeva, R. K., Bolotina, N. B., Sapozhnikov, A. N., Kashaev, A. A., Schoenleber, A. & Chapuis, G. (2002). *Crystallogr. Rep.* **47**, 404–407.

Sakamoto, S., Shimobayashi, N. & Kitamura, M. (2003). *Am. Mineral.* **88**, 1605–1607.

Sanchez-Munoz, L., Nistor, L., Van Tendeloo, G. & Sanz, J. (1998). *J. Electron Microsc.* **47**, 17–28.

Schutte, W. J. & de Boer, J. L. (1988). *Acta Cryst.* B**44**, 486–494.

Schutte, W. J. & de Boer, J. L. (1993). *Acta Cryst.* B**49**, 398–403.

Shannon, R. D. (1976). *Acta Cryst.* A**32**, 751–767.

Smaalen, S. van (2007). *Incommensurate Crystallography*. Oxford University Press.

Steurer, W. & Jagodzinski, H. (1988). *Acta Cryst.* B**44**, 344–351.

Subramanian, R. K., Muntean, L., Norcross, J. A. & Ailion, D. C. (2000). *Phys. Rev. B*, **61**, 996–1002.

Wilson, A. J. C. (1992). Editor. *International Tables for X-ray Crystallography*, Vol. C. Dordrecht: Kluwer Academic Publishers.

Withers, R., Noren, L., Welberry, T., Bindi, L., Evain, M. & Menchetti, S. (2008). *Solid State Ionics*, **179**, 2080–2089.

Withers, R. L., Thompson, J. G., Melnitchenko, A. & Palethorpe, S. R. (1998). *Acta Cryst.* B**54**, 547–557.

Xu, H. & Veblen, D. R. (1995). *Am. Mineral.* **80**, 87–93.

Yamamoto, A., Nakazawa, H., Kitamura, M. & Morimoto, N. (1984). *Acta Cryst.* B**40**, 228–237.